Time-Frequency Analysis based Motion Detection in Perfusion Weighted MRI

Sushma M
CVIT, IIIT Hyderabad, India
sushma.m@research.iiit.ac.in

Anubha Gupta
SPCRC, IIIT Hyderabad, India
agupta@iiit.ac.in

Jayanthi Sivaswamy
CVIT, IIIT Hyderabad, India
jsivaswamy@iiit.ac.in

***Abstract*—In this paper, we present a novel automated method to detect motion in perfusion weighted images (PWI), which is a type of magnetic resonance imaging (MRI). In PWI, blood perfusion is measured by injecting an exogenous tracer called bolus into the blood flow of a patient and then tracking it in the brain. PWI requires a long data acquisition time to form a time series of volumes. Hence, motion occurs due to patient's unavoidable movements during a scan, which in turn results into motion corrupted data. There is a necessity of detection of these motion artifacts on captured data for correct disease diagnosis. In PWI, intensity profile gets disturbed due to occurrence of motion and/or bolus passage through the blood vessels. There is no way to distinguish between motion occurrence and bolus passage. In this paper, we propose an efficient time-frequency analysis based motion detection method. We show that proposed method is computationally inexpensive and fast. This method is evaluated on a DSC-MRI sequence with simulated motion of different degrees. We show that our approach detects motion in a few seconds.**

I. Introduction

MRI has been emerging as an efficient tool in clinical practice for the analysis of brain functions through several metabolic parameters. There are two types of MRI, namely, diffusion weighted imaging (DWI) and perfusion weighted imaging (PWI). PWI has been used extensively for the evaluation of tissue after acute stroke, noninvasive histologic assessment of tumors and evaluation of neurodegenerative conditions such as Alzheimers disease [1]. There are two types of PWI: (i) dynamic susceptibility contrast (DSC) $T2^*$ imaging, and (ii) dynamic contrast enhanced (DCE) $T1$ weighted imaging. DSC is most widely used for the brain, while DCE is most widely used in the rest of the body though its experimental and research use is increasing in brain. In PWI, cerebral perfusion is used as a metabolic parameter, which explains the blood passage through the vascular system of the brain. An exogenous tracer called bolus is injected into the blood flow of a patient and then cerebral perfusion is measured by the analysis of hemodynamic time-to-signal intensity curve generated when bolus passes through the brain.

In PWI, a time series of volumes are formed in a long acquisition time. Patient often has difficulty in staying still during this period. Therefore, it is more likely that patient may move unavoidably during scanning which in turn results into motion artifacts in scans. There is a need of detection and subsequent correction of these motion artifacts. There are works in medical imaging, for example [2], [3], [4] addressed this problem in terms of registration of whole time series to a reference volume. These methods do not detect motion. Hence, non-corrupted volumes are also registered which makes the process computationally expensive and it is obvious that these volumes do not need any correction [5]. Therefore, it is preferable to have a prior knowledge about motion corrupted volumes.

In perfusion weighted MRI, intensity profile over time should be flat. If there are any disturbances in intensity profile, it can be due to two reasons: (i) passage of bolus through the blood vessels and (ii) motion of the patient during scanning. Therefore, while detecting motion, bolus passage should also be taken care of. However, traditional motion detection methods consider non-uniform intensity variations due to bolus passage as motion corruption. Hence, they may fail to detect motion in perfusion MRI. In [5] and [6], motion is detected by bolus dependent approach. Here, perfusion MRI data is divided into three sets as (i) pre wash-in, (ii) transit and (iii) post wash-out sets. Intensity correction is applied to transit set and then motion is corrected in each set differently. In this paper, we detect motion using time-frequency analysis.

Even though MRI scans consist of volumes of two dimensional images, they are acquired over the time. Therefore, we can extract one dimensional time series from volumes. Motion detection using one dimensional time series is obviously faster compared to that of two dimensional scans. These facts motivated us to analyze the MRI data in terms of one dimensional time sequences because we believe that frequency of time series will vary when there are motion artifacts. Most popular approach for temporal analysis is Fourier transform. Even though Fourier transform gives the information about the spectral components in a signal, it fails to locate where those frequencies occur in that signal. So, it is preferable to consider time frequency representation (TFR). Different techniques for time frequency representation have been proposed. A few of them are short time Fourier transform (STFT), Gabor transform, continuous wavelet transform (CWT) and Wigner ville distribution etc. In [7], it was proven that Stockwell transform (ST) outperforms all these TFR techniques in localizing time and frequency because it has frequency dependent resolution whereas other transforms have windows of fixed width. ST provides useful phase of the spectrum which is not available from CWT.

In the recent past, ST has been used for the analysis of MRI data. In [8], ST is used to remove artifacts in functional MRI (fMRI) time courses due to which brain activity detection is improved. In [9], polar version of ST is used to analyze the texture patterns in MRI for the diagnosis of multiple sclerosis. [10] discusses the effectiveness of ST for medical

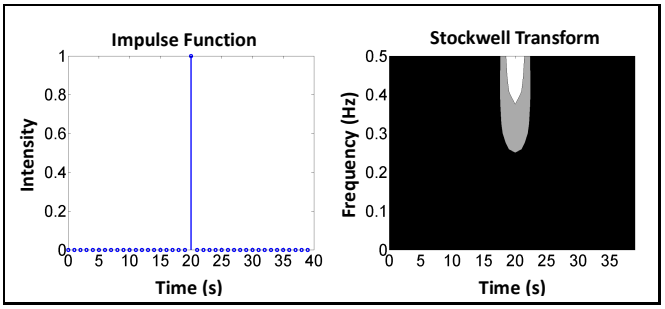

Fig. 1. Stockwell transform for an impulse function. Impulse function shown in left is $h[0:39]=0, h[20]=1$. Stockwell transform is shown in right. Note that bright pixels indicate high strength of transform. Here, bright pixels are at $t=20$.

imaging and shows how to enhance fMRI time courses by removing frequency artifacts which are introduced due to patient's quick breathing.

In this paper, we demonstrate how one dimensional ST can be used to detect motion. Given a MRI sequence of volumes, we consider specific key points which are generated by an automated method. Time series are extracted at these key points and ST is applied on them. The process is computationally inexpensive due to the facts that (i) motion is detected by one dimensional time series instead of two dimensional scans and (ii) these time series are extracted only at a few key points. Mean time taken for motion detection is around 3 seconds.

II. Stockwell Transform

In this section, we discuss details of Stockwell transform (ST) and its suitability for analyzing MRI time sequences. For a given time signal $h(t)$, its Stockwell transform is defined as,

$$S(\tau,f)=\int_{-\infty}^{\infty}h(t)w(\tau-t,f)e^{-i2\pi ft}dt \tag{1}$$

where $w(t,f)$ is defined as

$$w(t,f)=\frac{|f|}{\sqrt{2\pi}}e^{-t^2f^2/2}, \tag{2}$$

$h(t)$ is the time signal, $w(t,f)$ denotes the window, f denotes the frequency, τ denotes time shift parameter, and $|.|$ denotes absolute value. Since window ($w(t,f)$) is frequency dependent, narrower windows are applied at higher frequencies and broader windows are applied at lower frequencies. Hence, ST is a suitable time-frequency representation for current work.

In our work, intensity profiles over time are obtained from DSC-MRI sequence. There are strong disturbances in these one dimensional time series (intensity profiles) corresponding to motion corrupted volumes. In general, there will be many disturbances in time series with respect to number of continuous corrupted slices in MRI sequence. Since ST is a linear function, we explain it with one single intensity disturbance for simplicity. To show that these intensity variations are well represented by Stockwell transform, we modelled single disturbance in time series as an impulse, $h(t)$ as shown in Eq. 3.

$$h(t)=\delta(t-a) \tag{3}$$

ST of $h(t)$ is given as

$$S(\tau,f)=\frac{|f|}{\sqrt{2\pi}}e^{-(\tau-a)^2f^2/2}e^{-i2\pi fa} \tag{4}$$

Absolute value of $S(\tau,f)$ is given as

$$|S(\tau,f)|=\frac{f}{\sqrt{2\pi}}e^{-(\tau-a)^2f^2/2} \tag{5}$$

On taking first and second derivatives of Eq. 5 w.r.t. τ, we obtain

$$\frac{\partial|S(\tau,f)|}{\partial\tau}=-\frac{f^3}{\sqrt{2\pi}}(\tau-a)e^{-(\tau-a)^2f^2/2} \tag{6}$$

$$\frac{\partial^2|S(\tau,f)|}{\partial\tau^2}=\frac{f^3}{\sqrt{2\pi}}e^{-(\tau-a)^2f^2/2}[-1+f^2(\tau-a)^2] \tag{7}$$

In Eq. 5, $|f|$ is replaced with f because $f>0$. It can be easily observed that maximum of $|S(\tau,f)|$ occurs at $t=a$ because $\frac{\partial|S(\tau,f)|}{\partial\tau}\Big|_{\tau=a}=0$ and $\frac{\partial^2|S(\tau,f)|}{\partial\tau^2}\Big|_{\tau=a}<0$. Stockwell transform for $h(t)=\delta(t-a)$ with $a=20$ is shown in Figure 1. There is bright region around $t=20$ in ST. Even though there is some noise present in the time series, it does not affect ST much because the region around $t=20$ will still be bright relative to other regions.

III. Motion Detection

We propose a novel automated method to detect motion corrupted volumes in perfusion weighted MRI using Stockwell transform. We assume that there is no intra-volume motion in this MRI time series because it takes a few seconds time to scan. Therefore, whole volume is corrupted by same motion. Instead of considering whole volumes to detect motion, we consider only central slice of each volume. Motion can be identified through two ways, i.e., (i) intensity of voxel gets changed and (ii) a voxel comes into the location of another voxel. In this work, we detect motion using first category.

Overview of the proposed method to detect motion is shown in Fig. 2. For a given PWI MRI volume series, we consider central slices to detect the motion in corresponding volumes. The proposed method consists of the following steps: (i) Pre-processing, (ii) Estimation of landmark pixels, (iii) Time-frequency analysis of time series extracted at these landmark pixels, and (iv) Detection of locations of corrupted slices from time frequency representation of the extracted time series.

Algorithm for proposed motion detection method can be seen in Algorithm 1. If given PWI MRI series contains N volumes, there will be corresponding N central slices, $\{C_t\}_{t=1}^{N}$. Each central slice is of size $A\times B$. We first process all N central slices using intensity based thresholding technique such that the noise regions are discarded while preserving the edges. These pre-processed images, $\{I_t\}_{t=1}^{N}$, are then used to detect the motion. To determine the landmark pixels, it was observed that considering all pixels for detecting the motion corrupted slices is not efficient due to the fact that (i) the whole process will be time consuming and (ii) all pixels may not contain information about the corruption. Therefore, we adopted a mechanism to find landmark pixels. These pixels are obtained from the difference of consecutive central

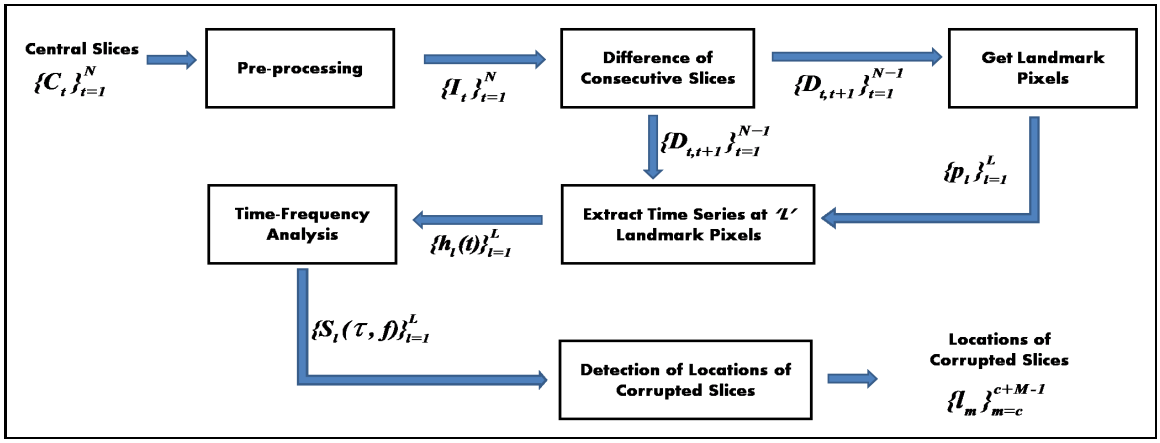

Fig. 2. Motion Detection. Central slices $\left(\{C_t\}_{t=1}^{N}\right)$ of a PWI MRI series are pre-processed to get noise-free images $\left(\{I_t\}_{t=1}^{N}\right)$. Then, one dimensional time series $\left(\{h_l(t)\}_{l=1}^{L}\right)$ at landmark pixels $\left(\{p_l\}_{l=1}^{L}\right)$ are extracted from difference of consecutive pre-processed slices $\left(\{D_{t,t+1}\}_{t=1}^{N-1}\right)$. Time-frequency analysis $\left(\{S_l(\tau,f)\}_{l=1}^{L}\right)$ is used to determine the locations of corrupted slices $\left(\{l_m\}_{m=c}^{c+M-1}\right)$.

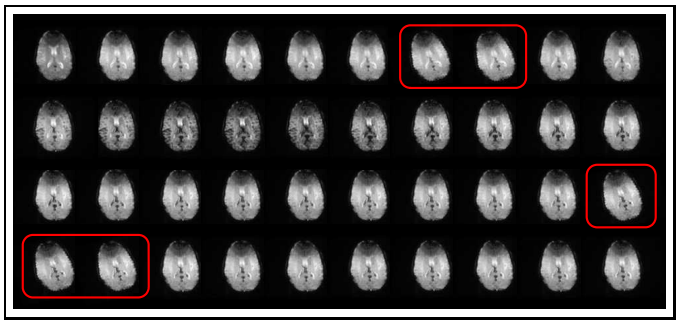

Fig. 3. DSC-MRI time series. It shows central slices of 40 volumes from top to bottom and left to right. Here, central slices corresponding to non-bolus phase are from 1 to 9 and from 21 to 40. -15^0 rotation is added to volumes 7, 8, 30, 31 and 32 respectively and their corresponding central slices are shown in red boxes.

slices $\left(\{D_{t,t+1}\}_{t=1}^{N-1}\right)$ of all given volumes because the pixels at edges definitely experience motion from one to another slice. All these edge difference maps are summed up and then landmark pixels, $\{p_l\}_{l=1}^{L}$, are selected such that every edge pixel can be considered. Then, one dimensional time series, $\{h_l(t)\}_{l=1}^{L}$, at all L landmark pixels are extracted from $\{D_{t,t+1}\}_{t=1}^{N-1}$.

Wherever motion occurs, there will be a strong disturbance at that slice location in one dimensional time series. Therefore, there may be many disturbances depending on the number of consecutive corrupted slices. It is difficult to find those consecutive slices from the time series itself. For this purpose, we use Stockwell transform $\left(\{S_l(\tau,f)\}_{l=1}^{L}\right)$ at all L extracted time series. There might be still a few of landmark pixels which may not represent the pixels that undergo motion. To take care of this, Stockwell transforms at all landmark pixels can be added to get proper representation so that non-significant landmarks can play negligible role in detecting motion. This summed up Stockwell transform can be denoted as, $S(\tau,f) = \sum_{l=1}^{L} S_l(\tau,f)$. As explained in Section II, there will be bright region at locations of corrupted slices. If there are M consecutive corrupted volumes, bright region will be around corresponding M locations in ST. We extract those bright regions and locations where those bright regions occur. If there is a bright region from location l_c to l_{c+M-1}, then we can categorize the slices at locations, $\{l_m\}_{m=c}^{c+M-1}$, as corrupted slices and corresponding volumes are motion corrupted.

IV. Experiments and Results

We have conducted experiments to validate the performance of the proposed framework with a DSC-MRI data obtained from a 1.5T GE MRI scanner. The data details are: number of volumes = 40 (1s/phase), number of slices = 20, dimensions of slice = 128x128 and thickness of slice = 5mm. All experiments are implemented on a system with 4GB RAM and Intel® core i5 CPU with 2.5 GHz processor.

There are 29 non-bolus volumes out of 40 volumes. Here, non-bolus volumes means volumes in which bolus is not present in brain. For our experiments, we introduced 3D rotation to DSC-MRI volumes to simulate motion in transverse plane in the range $[-20^0\ 20^0]$ in random number of volumes. We detect motion as explained in Section III. Table I shows the performance of our motion detection method with number of corrupted volumes as 5, 10, 20, and 25 respectively. These corrupted volumes are chosen randomly and they are not always consecutive volumes. This randomness reflects the worst possible scenarios during scanning. Here, we considered only rotation because translation inside the scanner is almost impossible due to the structure of MRI scanner. A specific case is shown in Fig. 3 where central slices of 5 volumes are corrupted by a rotation of -15^0. In general, different amount of rotation can be possible at different sets of consecutive volumes according to patient's typical movements. For example, as shown in Fig. 3, 7^{th}, 8^{th} volumes can be corrupted by a rotation of -15^0 while 30^{th}, 31^{st} and 32^{nd} volumes can be corrupted by a different amount of rotation other than 15^0. We have experimented with many such scenarios also and we are still able to achieve similar performance. It can be observed from Table I that except for the range $[-1^0\ 1^0]$, our method is able to detect all corrupted volumes correctly. Even in practical cases, there is less probability that patient can move only 1^0. In case of 25 corrupted volumes, we are able to detect all 25 for

TABLE I. EVALUATION OF PROPOSED MOTION DETECTION METHOD.

# Non-bolus/Total Volumes	29/40							
# Corrupted Volumes	5		10		20		25	
Simulated Rotation	# Detected Volumes	Time Taken (in sec)	# Detected Volumes	Time Taken (in sec)	# Detected Volumes	Time Taken (in sec)	# Detected Volumes	Time Taken (in sec)
$[-1^0\ 1^0]$	3	2.62	8	2.642	11	2.64	13	2.75
$[-5^0\ 5^0]$	5	2.622	10	2.642	20	2.67	25	2.81
$[-10^0\ 10^0]$	5	2.65	10	2.66	20	2.68	25	2.82
$[-15^0\ 15^0]$	5	2.67	10	2.78	20	2.87	25	2.93
$[-20^0\ 20^0]$	5	2.69	10	2.72	20	2.97	25	3.25

Algorithm 1 Motion Detection

Input: Central slices, $\{C_t(i,j)\}_{t=1}^{N}$ where $i = 1$ to A, $j = 1$ to B

1) *Pre-processing:*
   - Pre-process all central slices for removing the noise regions at edge regions to get $\{I_t(i,j)\}_{t=1}^{N}$

```
for t = 1 to N do
    I_t = C_t
    M_t = mean(C_t)
    for i = 1 to A do
        for j = 1 to B do
            if I_t(i,j) < M_t then
                I_t(i,j) = 0
            end if
        end for
    end for
end for
```

2) *Find locations of landmark pixels:*
   - Find difference of consecutive images, $\{D_{t,t+1}\}_{t=1}^{N-1}$

```
for t = 1 to N − 1 do
    D_{t,t+1} = |I_t − I_{t+1}|
end for
```

   - Find landmark pixels, $\{p_l\}_{l=1}^{L} = \{(x_l, y_l)\}_{j=1}^{L}$
3) *Extract time series:*
   - Extract time series $\{h_l(t)\}_{l=1}^{L}$ at locations $\{p_l\}_{l=1}^{L}$ from $\{D_{t,t+1}\}_{t=1}^{N-1}$

```
for j = 1 to L do
    for t = 1 to N − 1 do
        h_j(t) = D_{t,t+1}(x_l, y_l)
    end for
end for
```

4) *Determine Stockwell transform:*
   - Find Stockwell transform of each time series, $\{S_l(\tau, f)\}_{l=1}^{L}$

```
for l = 1 to L do
    S_l(τ, f) = ∫_{−∞}^{∞} h_j(t) w(τ − t, f) e^{−i2πft} dt
end for
```

5) *Estimation of locations of corrupted slices:*
   - Sum all STs, $S(\tau, f) = \sum_{j=1}^{L} S_j(\tau, f)$
   - Find locations of bright regions, l_c and l_{c+M-1}

Output: Locations of corrupted volumes, $\{l_m\}_{m=c}^{c+M-1}$

$[-10^0\ 10^0]$, $[-15^0\ 15^0]$ and $[-20^0\ 20^0]$, while in [6], 21, 24 and 22 volumes are detected for respective motions. Average of time taken for all experiments for each case are shown in Table I. Time taken to detect motion is around 3 seconds (see Table I) while it is from 7.68 to 132.21 seconds (depending on block size) in [5]. This reduction in time is due to the fact that proposed method detects motion using one dimensional time series instead of two dimensional images.

V. CONCLUSIONS AND FUTURE WORK

We have proposed a novel automated approach for motion detection in DSC-MRI perfusion data using time-frequency analysis. Instead of considering all two dimensional images for the process, we used one dimensional time series due to the fact that these scans are acquired over time. This made the proposed method computationally inexpensive. We have demonstrated that motion detection can be performed in automated fashion by using a time frequency representation called Stockwell transform. We demonstrated our method in non-bolus phase of perfusion MRI sequences. However, the proposed method will work in the bolus phase provided pre-processing is done to account for the local contrast change. In future, we look forward to extend this method to (i) detect motion in all possible directions (ii) detect bolus phases first and then motion and (iii) correct motion.

REFERENCES

[1] J. R. Petrella and J. M. Provenzale, "MR perfusion imaging of the brain: techniques and applications," *American Journal of Roentgenology*, vol. 175, no. 1, pp. 207–219, 2000.

[2] G. A. Buonaccorsi *et al.*, "Tracer kinetic model–driven registration for dynamic contrast-enhanced MRI time-series data," *Magnetic Resonance in Medicine*, vol. 58, no. 5, pp. 1010–1019, 2007.

[3] M. Jenkinson *et al.*, "Improved optimization for the robust and accurate linear registration and motion correction of brain images," *Neuroimage*, vol. 17, no. 2, pp. 825–841, 2002.

[4] T. R. Steger and E. F. Jackson, "Real-time motion detection of functional MRI data," *Journal of Applied Clinical Medical Physics*, vol. 5, no. 2, pp. 64–70, 2004.

[5] R. Gautam *et al.*, "A method for motion detection and categorization in perfusion weighted MRI," in *ICVGIP*, 2012, pp. 6:1–6:8.

[6] R. Gautam *et al.*, "An efficient, bolus-stage based method for motion correction in perfusion weighted MRI," in *ICPR*, 2012, pp. 145–148.

[7] R. G. Stockwell *et al.*, "Localization of the complex spectrum: the S transform," *IEEE Transactions on Signal Processing*, vol. 44, no. 4, pp. 998–1001, 1996.

[8] B. G. Goodyear *et al.*, "Removal of phase artifacts from fMRI data using a Stockwell transform filter improves brain activity detection," *Magnetic Resonance in Medicine*, vol. 51, no. 1, pp. 16–21, 2004.

[9] Y. Zhang, "MRI texture analysis in multiple sclerosis," *Journal of Biomedical Imaging*, vol. 2012, pp. 762–804, 2012.

[10] H. Zhu *et al.*, "A new local multiscale Fourier analysis for medical imaging," *Medical physics*, vol. 30, pp. 1134–1141, 2003.